

1

2 MR JERONYMO DALAPICOLLA (Orcid ID : 0000-0002-4819-9720)

3 MS. JOYCE RODRIGUES PRADO (Orcid ID : 0000-0002-2025-5479)

4 DR ALEXANDRE REIS PERCEQUILLO (Orcid ID : 0000-0002-7892-8912)

5

6

7 Article type : Research Article

8

9

This is the author manuscript accepted for publication and has undergone full peer review but has not been through the copyediting, typesetting, pagination and proofreading process, which may lead to differences between this version and the Version of Record. Please cite this article as doi: 10.1111/JBI.14281

This article is protected by copyright. All rights reserved

10 Type: **Research Article**

11

12 Title: **Functional connectivity in sympatric spiny rats reflects different dimensions of Amazonian forest-association**

13

14 Running Title: **Testing connectivity hypotheses**

15

16 Jeronimo Dalapicolla^{1,2*}, Joyce Rodrigues do Prado¹, Alexandre Reis Percequillo¹, L. Lacey Knowles³

17

18 ¹ Departamento de Ciências Biológicas, Escola Superior de Agricultura “Luiz de Queiroz”, Universidade de São Paulo, São
19 Paulo, Brazil.

20 ² Instituto Tecnológico Vale, Belém, Pará, Brazil.

21 ³ Department of Ecology and Evolutionary Biology, Museum of Zoology, University of Michigan, Ann Arbor, Michigan,
22 United States of America.

23

24 ***Corresponding author:** Jeronimo Dalapicolla. Departamento de Ciências Biológicas, Escola Superior de Agricultura
25 “Luiz de Queiroz”, Universidade de São Paulo, Av. Pádua Dias, 11 – Caixa Postal 9, Piracicaba, São Paulo, Brazil.

26 Present address: Instituto Tecnológico Vale, Rua Boaventura da Silva, 955, Nazaré, Belém, Pará, Brazil.

27

28 **Email:** jdalapicolla@gmail.com; jeronimo.dalapicolla@pq.itv.org

29 ACKNOWLEDGMENTS

30 To museums and mammal collections from Brazil, USA and their curators for the genetic samples: Eleanor Hoeger, Robert
31 Voss, Svetlana Katanova (AMNH-AMCC, New York, USA); Lauren Smith, Bruce D. Patterson (FMNH, Chicago, USA);
32 Mariel Campbell, Jonathan Dunnum, Joseph Cook (MSB, Albuquerque, USA); Chris Conroy, Eileen Lacey, James Patton
33 (MVZ, Berkeley, USA); Ismael de Jesus, Juliana Gualda, Mario de Vivo, Luiz Fábio Silveira (MZUSP, São Paulo, Brazil);
34 Alfred Gardner, Darrin Lunde, Indrid Rochon, Louise Emmons (NMNH, D.C., USA); Kathy MacDonald, Caleb Phillips
35 (TTU, Lubbock, USA). Carolina Carvalho, Jamille Veiga, Leonardo Trevelin, and Rodolfo Jaffé for comments and tips on
36 MLPE analyses. To Instituto Chico Mendes de Conservação da Biodiversidade (ICMBio) for issuing the collecting permits
37 required for this research (permission SISBIO n. 14419-3). The Knowles lab staff, especially Andrea Thomaz, Mariah
38 Kenney, Luciana Resende-Moreira, and Karina Amaral, for comments and tips on methods and analyses that improved the
39 manuscript's quality. This work was supported by the Fundação de Amparo à Pesquisa de São Paulo (FAPESP) [grant
40 numbers 09/16009-1, 15/02853-6, 16/24464-4, 16/20055-2]; J.D. received initial scholarship from the Coordenação de
41 Aperfeiçoamento de Pessoal de Nível Superior (CAPES), grant from the American Museum of Natural History (AMNH –
42 Collection Study Grant), and currently a PD scholarship from Instituto Tecnológico Vale (ITV).

43

44 SIGNIFICANCE STATEMENT

45 We investigate how habitat heterogeneity affects divergence processes and compare these processes between sympatric
46 rodent species across the vast geographic area of the Western Amazon. This study appeals to the broad readership given the
47 themes of landscape genomics analyses in relation to habitat heterogeneity, as well as tests of how differences in habitat
48 associations in little-studied area employing taxa of the Amazon's seasonal floodplain forests (*várzea*) and non-flooded
49 forests (*terra-firme*).

50

51 CONFLICT OF INTEREST STATEMENT

52 The authors declare no conflicts of interest.

53 **ABSTRACT**

54 **Aim:** Understanding how the landscape influences gene flow is important in explaining biodiversity, especially when co-
55 distributed taxa across heterogeneous landscapes exhibit species-specific habitat associations. Here, we test predictions
56 about the effects of forest-type on population connectivity in two sympatric species of spiny rats that differ in their forest
57 associations. Specifically, we evaluate the hypothesis that seasonal floodplain forests (*várzea*) provide linear connectivity,
58 facilitating gene flow among individuals, while non-flooded forests (*terra-firme*) may diminish the functional connectivity.

59
60 **Location:** Western Amazon, South America.

61
62 **Taxon:** *Proechimys simonsi* (non-flooded forests, *terra-firme*) and *Proechimys steerei* (seasonal floodplain forests, *várzea*).

63
64 **Methods:** We analyze about 13,000 SNPs along with characterizations of landscape heterogeneity for two forest types to
65 test for differences in the functional connectivity. Influence of the landscape and environmental variables are quantified
66 using maximum-likelihood population effect (MLPE) models to identify the relative importance of variables in explaining
67 the gene flow.

68
69 **Results:** There are significant differences in functional connectivity between species. However, the genomic data does not
70 support the conventional hypotheses of higher connectivity for inhabitants of *várzea* than those of *terra-firme*. Stronger
71 genetic structure in *P. steerei* than *P. simonsi* based on IBD models suggests reduced gene flow in species associated with
72 *várzea* forests. Isolation by resistance reinforces that wetland habitats inhibit and promote the functional connectivity in *P.*
73 *simonsi* and *P. steerei*, respectively, although large distances along the rivers can prevent gene flow in *P. steerei*.

74
75 **Main conclusions:** Interpreting differences between connectivity in taxa apparent from genetic analyses through the lens of
76 a single dimension of Amazonian heterogeneity – that is, forest type – may be an oversimplification. Our statistical
77 modeling and fit of the data to different models points to specific environmental and habitat differences between the
78 ecological divergent spiny rat species that may contribute to differences in the genetic structure of these sympatric taxa.

79
80 **KEYWORDS:** Isolation by resistance; Landscape genetics; MLPE mixed models; Phylogeography; RADseq; *Terra-firme*;
81 *Várzea*.

82 1. INTRODUCTION

83 Landscape configuration and composition can influence gene flow among populations (Manel et al., 2003) such
84 that organisms with different ecologies can show different connectivity patterns in the same landscape (Balkenhol et al.,
85 2015). The effects of the landscape on the dispersal of organisms are understood as functional connectivity, given that it's
86 not geographic distance alone that determines gene flow, but also how organisms perceive and respond to landscape
87 structure (Manel & Holderegger, 2013). As such, the divergence process may differ among sympatric taxa when the
88 species' ecologies affect connectivity among populations because of differences in how they perceive and respond to the
89 landscape (Pirani et al., 2019), in addition to differences in the landscape structure of different habitat types (Massatti &
90 Knowles, 2016; Prado et al., 2019).

91 Restrictive factors in a landscape may prevent movement and connection of the organisms (Taylor et al., 1993)
92 through *i*) Isolation by Resistance (IBR), where restrictions are based on landscape structure and configuration (McRae,
93 2006), or *ii*) Isolation by Distance (IBD), where geographical distance determines the amount of dispersal (Wright, 1943).
94 Connections (or conversely isolation) between populations can relate to historical processes, such as vicariance and
95 dispersion events (Carnaval & Moritz, 2008; Ribas et al., 2012), or reflect ecological and behavioral traits (e.g., mating
96 patterns, migration capacity, habitat use), which may create resistance or facilitate organisms movements across
97 heterogeneous landscapes and environments and generate different patterns of local adaptation, genetic diversity, and
98 population structure (McRae & Beier, 2007).

99 Studies focusing on functional connectivity, gene flow, and genetic diversity are important to explain biodiversity
100 patterns, as well as to provide important information for conservation biology (Hoban et al., 2020), especially in poorly
101 known environments, such as the Western Amazon (Barlow et al., 2016). Bordered by the Andean slopes to the west and
102 the Negro River and Madeira River to the east (Leite & Rogers, 2013), the Western Amazon has a dynamic geological
103 history unlike the rest of the Amazon and a unique river dynamic of meandering white-water rivers and seasonal floods
104 (Hoorn et al., 2010; Matocq et al., 2000). Western Amazonian landscape is predominated by two dominant forest types:
105 non-flooded or *terra-firme* forests, and seasonal floodplain forests or *várzea* forests. The non-flooded forests are above the
106 maximum flood level of rivers and perennial streams, and it abuts the seasonally inundated floodplains forests (Bredin et al.,
107 2020). As non-flooded systems, except for the occasional minor inundation of flood water (Hess et al., 2015), inhabitants of
108 the *terra-firme* forests are hypothesized to experience greater stability, and hence are expected to be characterized by higher
109 genetic diversity, compared with inhabitants of the floodplain forests (Harvey et al., 2017). On the other hand, seasonal
110 flooding of *várzea* forests produce a dynamic of meandering river channels (Constantine et al., 2014) in which sections of
111 land frequently move from one river side to the other, and as such, are hypothesized to facilitate gene flow among the
112 populations of the inhabitants of this forest (Salo et al., 1986; Matocq et al., 2000) via connectivity along the floodplains
113 bordering rivers, as well as by temporary dispersal corridors between river basins during seasonal flooding of the *várzea*
114 forests. This general framework has been supported by genetic studies of different members of the communities that inhabit
115 the *várzea* forests, including species of birds (Aleixo, 2006; Cadena et al., 2011; Harvey et al., 2017), plants (Godoy et al.,
116 1999) and mammals (Matocq et al., 2000). However, questions remain about the extent to which this hypothesis can be
117 generalized, especially in organisms with different dispersal characteristics (see Thom et al., 2020).

118 Among the species-rich fauna that inhabits the non-flooded and seasonal floodplain forests of the Western
119 Amazon (Voss & Emmons, 1996), the diversity of rodents stands out among mammals, especially the genus *Proechimys* J.
120 A. Allen, a terrestrial spiny rat of the family Echimyidae (Fabre et al., 2016). With a wide Neotropical distribution that

121 extends from Central America to the Brazilian Cerrado, covering the entire Amazon region (Patton & Leite, 2015; Woods &
122 Kilpatrick, 2005), nine of the 22 species in the genus are found in the Western Amazon (Fabre et al., 2016; Patton & Leite,
123 2015). Within Western Amazon, records of sympatry (i.e., overlapping geographic distributions) and syntopy (i.e.,
124 overlapping collection sites) have also been documented for up to five species of *Proechimys* (Patton et al., 2000). Thus,
125 sympatry among species of *Proechimys* is both more common and occurs across more species compared with other
126 mammal taxa that occur sympatrically (Patton & Leite, 2015), as in the Atlantic Forest echimyid genera *Phyllomys* (Leite,
127 2003) and *Trinomys* (Lara & Patton, 2000). This is an unusual pattern, as most co-generic Neotropical rodent species are
128 predominantly allopatric and/or parapatric (Patton et al., 2015). Differences in their ecology, including different habitat
129 preferences are factors frequently invoked to explain the overlapping distributional patterns of *Proechimys* species
130 (Emmons, 1982; Matocq et al., 2000; Patton et al., 2000; Voss et al., 2001). However, the potential explanations for the
131 disproportionate occurrence of sympatry (i.e., divergent ecologies) have yet to be examined with regards to their
132 consequences for the divergence process among sympatric taxa.

133 Here, we address this knowledge gap by testing how the pattern of connectivity within two sympatric species, *P.*
134 *simonsi* and *P. steerei*, may differ in relation to the type of forest each inhabits (non-flooded versus flooded). *P. simonsi*
135 primarily inhabits upland and relatively stable non-flooded forest (*terra-firme*) environments surrounded by flooded areas
136 (Patton et al. 2000; Patton & Leite, 2015), whereas *P. steerei* occurs in the seasonal floodplain (*várzea*) and in higher areas
137 within *várzeas* called *restingas* during seasonal floods or secondarily in disturbed *terra-firme* forests adjoining flooded areas
138 (Matocq et al., 2000; Patton & Leite, 2015). Analyses of mitochondrial DNA (mtDNA) of individuals along the Juruá River
139 suggested that gene flow differs between the species and is consistent with general expectations based on their forest type
140 association (i.e. *P. simonsi* presented lower levels of gene flow than *P. steerei*; Matocq et al., 2000). However, there were
141 some notable peculiarities. Specifically, mtDNA genetic structure is stronger among headwaters areas than lower river areas
142 and is more pronounced in *P. steerei* than *P. simonsi* (Matocq et al., 2000), leading the authors to speculate that landscape
143 features of the Juruá River, and possibly aspects of the species natural history traits, contributed to the counter-intuitive
144 differences in the geographic structure of mtDNA between these species.

145 In this study, we overcome the limitations of single locus analyses by collecting genomic data from individuals
146 sampled from multiple rivers across western Amazon to avoid site (or river) specific affects. As such, our study applies a
147 comparative framework to address the generality of predictions about the effects of forest-type on population connectivity
148 using analytical techniques to test if gene flow corresponds to expectations about functional connectivity. Specifically, and
149 taking into account the mtDNA findings (Matocq et al., 2000), we evaluate support for the hypothesis that seasonal
150 floodplain forests provide linear connectivity, facilitating gene flow among *P. steerei* individuals. However, considering the
151 unexpectedly strong genetic structure of mtDNA in *P. steerei*, relative to *P. simonsi* (Matocq et al., 2000), we also test a
152 suite of models that differ in the landscape features they contain to explore how particular factors may potentially restrict
153 gene flow in each spiny rat taxa. As such, our study moves beyond relying solely on concordance, or the lack-there-of,
154 among taxa as a typical means for evaluating hypotheses about the effects of species-specific traits on gene flow (see
155 Papadopoulou & Knowles, 2016). We discuss the implications of our results for understanding how the divergence process
156 may differ because of species-specific ecologies (i.e., inhabiting non-flooded or *terra-firme* forests versus seasonal
157 floodplain forests or *várzea* forests) of Amazonian taxa, as well as potential linkages with the high biodiversity of the
158 Western Amazon biome.

159

160 2. MATERIAL AND METHODS

161 2.1. Genomic data

162 Genomic data was collected from 41 individuals of two co-distributed species of spiny rats: *P. simonsi* ($n = 21$), which
 163 inhabits non-flooded forests (*terra-firme*), and *P. steerei* ($n = 20$), which occupies seasonal floodplain forests (*várzea*) from
 164 the Western Amazon (Fig. 1). Note that sampling in the Western Amazon, as well as from different countries, is inherently
 165 difficult, and even more so for focused collections of co-distributed species, which limits the attainable sample sizes.
 166 Nevertheless, our sampling covers most of the distribution of each species, including areas of sympatry (Fig. 1), and we
 167 note that the small sample sizes are compensated to some extent by more than 10,000 SNPs sequenced with good coverage
 168 ($> 30X$) for each species (see Li et al., 2020; McLaughlin & Winker, 2020; Nazareno et al., 2017).

169 Individuals were collected by the Laboratório de Mamíferos (Universidade de São Paulo) following the American
 170 Society of Mammalogists guidelines (Sikes et al., 2016) and the Brazilian legislation (permission SISBIO n. 14419-3) and
 171 are housed at the Coleção de Mamíferos da Escola Superior de Agricultura “Luiz de Queiroz, Universidade de São Paulo,
 172 Piracicaba, São Paulo, Brazil (LMUSP). In addition, some samples were obtained from several scientific collections (see
 173 Appendix S1 in Supporting Information: Table S1.1). Specimens were identified using morphologic diagnostic traits
 174 (described in Patton & Leite, 2015). One double digest Restriction-site Associated DNA (ddRAD) library was constructed
 175 following Peterson et al. (2012) protocol, generating 150 bp reads where one SNP was randomly selected per locus. More
 176 details about DNA extraction and library preparation, SNPs calling and filtering steps, see Appendix S2.1 in Supporting
 177 Information.

179 2.2. Genetic structure and genetic diversity

180 Genetic structure in both species was evaluated using three different model-free approaches: *i*) sparse non-
 181 Negative Matrix Factorization algorithms (sNMF) using “LEA” v3.4.0 (Frichot & Francois, 2014), *ii*) Discriminant
 182 Analysis of Principal Component (DAPC) using “adegenet” v2.1.3 (Jombart & Ahmed, 2011), and *iii*) Principal
 183 Component Analysis (PCA) using *dudi.pca* function in “adegenet” followed by Tracy-Widom tests for eigenvalues to select
 184 significant PCs (Patterson et al., 2006; Tracy & Widom, 1994). This set of analyses was chosen because of their
 185 complementarity. Specifically, as the most common method in population genomics that allows reduction of the complexity
 186 of genomic data while preserving its covariance, PCA were conducted. However, given PCA’s sensitivity to sample size,
 187 missing data, number of loci, presence of clines, and isolation by distance (Puechmaille, 2016), we used more than one
 188 method to estimate genetic structure. In particular, as model-free approaches, DAPC and sNMF do not require population
 189 genetics assumptions (such as HWE, linkage disequilibrium, and others), are computationally fast for genome-scale data,
 190 and do not require *a priori* definition of genetic groups. DAPC has proven effective even in complex population structures
 191 such as clines and hierarchical groups (Fenderson et al., 2020; Jombart et al., 2010). sNMF is similar to, but much faster
 192 than, STRUCTURE and ADMIXTURE for calculating ancestry coefficients (which DAPC and PCA do not) when
 193 estimating genetic clusters (Frichot et al., 2014).

194 Ten replicates of each K -value, for K of 1 to 10 potential genetic clusters were run for the sNMF analyses with
 195 different regularization parameters values ($\alpha = 10, 100, 500, 1000, 2000, 4000$) following Dalapicolla et al. (2021); the best
 196 K was estimated applying a minimum cross-entropy value (Frichot et al., 2014). For the DAPC, genetic clusters (K)
 197 between 1 and 10 were tested using all PCs (100% of the variance); the Bayesian Information Criterion (BIC) with the
 198 function *find.clusters* (Jombart et al., 2010; Miller et al., 2020) in “adegenet” was used to identify the best K (i.e., the one

199 with the lowest value, as with the cross-entropy evaluation). The *xvalDapc* function in “adegenet” was used to select the
 200 best number of PCs to recover genetic clusters (Miller et al., 2020).

201 The following genetic diversity metrics were calculated for each genetic cluster identified in each species:
 202 expected heterozygosity (HE_{EXP}), nucleotide diversity (π), and inbreeding coefficient (F_{IS}), using the *Query* function
 203 available in “r2vcftools” v0.0.0.9 (Pope, 2020). Tests of significant differences in diversity values (among species and
 204 among genetic clusters) were assessed with Tukey’s test using *Query* function as well (see Prado et al., 2019). In addition,
 205 F_{ST} (SNP-based F -statistics) was used to measure genetic differentiation between genetic clusters using the *gl.fst.pop*
 206 function in “dartR” v1.9.9.1 (Gruber & Georges, 2019) with 100 bootstraps. All analyses were performed in R 3.6.3 (R
 207 Core Team, 2020).

208

209 2.3. Isolation by distance (IBD)

210 The association between geographic and genetic distance was tested using Mantel tests (Mantel, 1967) based on *i*) a
 211 geographic (Euclidean) distance matrix and *ii*) a river network distance along the main river channels, using the *mantel.rtest*
 212 function with 10,000 permutations in “ade4” v1.7-16 (Dray & Dufour, 2007); details on environmental distances are given
 213 in Appendix 2.2. A genetic PCA-distance between individuals was calculated using *distance* function in “ecodist” v2.0.7
 214 (Goslee & Urban, 2007) based on the Euclidean distance, retaining the number of PCs according to the Broke Stick Rule in
 215 *screenplot* function in “vegan” v2.5-7 (Oksanen et al., 2019); this metric was used because of its performance for IDB tests
 216 when sample sizes differ (Shirk et al., 2017) and it can be interpreted similarly to F_{ST} used in classical population-based
 217 Mantel tests. An analysis of covariance (ANCOVA) was performed to test if the slopes of the Mantel tests differed between
 218 species. Robustness was examined by sequential elimination and replacement of each genetic cluster (i.e., verifying whether
 219 the correlation and significance values were dependent on any specific genetic cluster). Procrustes analyses were also used
 220 to test the similarity between taxa in the structuring of genetic variation, under the expectations of isolation by distance
 221 (IBD) (Knowles et al., 2016). The associations tests between genetic variation and geography was quantified using the
 222 *protest* function in “vegan” package, see details for this methodology in Appendix S2.2. All analyses were performed in R
 223 3.6.3.

224 2.4. Isolation by Resistance (IBR)

225 Isolation by Resistance (IBR) analyses were conducted using Maximum Likelihood population effects (MLPE)
 226 mixed models (Clarke et al., 2002), and are more accurate for individual-based evaluation of functional connectivity on
 227 landscape (Shirk et al., 2018). Yang’s relatedness coefficient (Yang et al., 2010), estimated in “r2vcftools” using the
 228 *Relatedness* function, was used as the response variable in the MLPE models because relatedness coefficients are more
 229 likely to represent recent gene flow (Balkenhol et al., 2015; Carvalho et al., 2019) and it is commonly applied for IBR tests
 230 based on individual-based genetic distances (Jaffé et al., 2019; Shirk et al., 2017). Mixed-effects regression models and least
 231 squares penalization with correlation structure were applied to account for the non-independence of genetic pairwise
 232 distances (Clarke et al., 2002), using the function *lme* in “nlme” v3.1-152 (Pinheiro et al., 2020) and the “corMLPE” v0.0.3
 233 package (<https://github.com/nspope/corMLPE>). A random effect specifying pairwise distances of individuals from the same
 234 versus different genetic clusters was used to control for population structure (Carvalho et al., 2019). Specifically, a full
 235 model containing all possible combinations among the predictors was fit to the genetic distances, considering five different
 236 resistance matrices as predictors: *i*) the null model based on geographic (Euclidean) distance (which we expect will not be
 237 significant predictor/component for any IBR models if landscape features are important to functional connectivity), and four

238 matrices representing environmental differences between non-flooded (*terra-firme*) forests and seasonal floodplain forests
 239 (*várzea*) (Table S1.2): *ii*) topographic distance; *iii*) river network distance; *iv*) habitat productivity distance (a resistance
 240 layer created from species distribution models, SDM, in which temperature, precipitation, and potential evapotranspiration
 241 (PET) variables act as a habitat productivity proxy (Hawkins et al., 2003; Li et al., 2011, see Appendix S2.2 and see
 242 Appendix S3: Fig S3.1) using presence-only data for both species (Table S1.3), and *v*) habitat resistance based on a
 243 wetlands map for the Western Amazon (Gumbrecht et al., 2017), which represent movements within a landscape based on
 244 habitat preferences. Resolution for all raster variables was 30 arc-sec (~1Km² per cell), except for the wetlands raster that
 245 was resampled from the original spatial resolution (231 m²) using *resample* function from “raster” v3.4-10 (Hijmans & van
 246 Etten, 2015). All values in the resistance matrices were set to greater than zero to avoid errors in the model analyses (i.e., 0
 247 values were replaced with 0.001). The set of 4 variables incorporated into the competing models were chosen to capture
 248 aspects of the non-flooded (*terra-firme*) and seasonal floodplain (*várzea*) forests that differ, and hence, may result in
 249 dispersal differences in their respective inhabitants. For example, topographic distance was included because we expect
 250 species will avoid movements between different forest types, and hence altitudes. Likewise, river network distance might be
 251 a critical predictor for the seasonal floodplain inhabitants (i.e., *P. steerei*), with *várzea* forests acting as a dispersal corridor
 252 along rivers. As with topographic distance, habitat productivity distance was included as a potential significant predictor of
 253 gene flow in both species because individuals are expected to disperse more commonly between areas with similar habitat
 254 productivity, given that productivity of seasonal floodplain forests (*várzea*) and non-flooded forest (*terra-firme*) are distinct
 255 (Junk & Piedade, 1993; Wittmann et al., 2010). Lastly, habitat resistance represents differential movements of the species
 256 based on habitat preferences and direct measures of habitat type. Specifically, the *P. steerei* the resistance matrix was built
 257 such that wetlands facilitated dispersal, whereas for *P. simonsi* the resistance matrix was built with wetlands posing greater
 258 resistance to gene flow (see Appendix 2.2 and Table S1.4). If forest-types are important to functional connectivity in both
 259 species, this predictor will be significant in both species as well. Methodological details on the methodologies for
 260 calculating all resistance matrices are given in Appendix S2.2.

261 To avoid models containing highly correlated predictors, we eliminated models with highly correlated predictors
 262 (i.e., $r^2 > 0.6$; Fig. S3.2; see also Castilla et al., 2020; Jaffé et al., 2019; Rutten et al., 2019) using the *dredge* function from
 263 “MuMIn” v1.43.17 (https://github.com/rojaff/dredge_mc). The retained models generated in this approach therefore contain
 264 all potential predictors, as opposed to an approach of *a priori* removal of correlated predictors with the highest variance
 265 inflation factor for identifying models without highly correlated predictors.

266 The best IBR models ($\Delta AIC < 2$) were identified (Harrison et al., 2018), with confidence intervals for
 267 coefficients of association estimated using restricted maximum likelihood (REML method; Silk et al., 2020). Spatial
 268 dependence of residuals from these models was evaluated by *acf* function in “stats” v3.6.3 (Castilla et al., 2020; Jaffé et al.,
 269 2019). Likelihood ratio tests (LRT) were used to identify the best model among the nested models using the *anova.lme*
 270 function in the “nlme”, and the significance of predictors were estimated by chi-squared contingency table tests, using
 271 *drop1* function in “stats”. Conditional coefficients of determination (conditional R^2) for quantifying the variation explained
 272 by the model was calculated in “MuMIn” (Nakagawa & Schielzeth, 2013), and the semi partial R^2 that measures the
 273 proportion of variance explained by each predictor (Jaeger et al., 2017) were estimated with the *r2beta* function in the
 274 “r2glmm” v0.1.2 (Jaeger, 2017). The relative importance of each predictor in explaining functional connectivity was
 275 determined by summing AIC weights over all models with $\Delta AIC < 2$ using functions *get.models* and *importance* in R
 276 package “MuMIn”. All analyses were performed in R 3.6.3.

277

278

279 **3. RESULTS**

280 After processing the raw sequence reads and applying stringent filtering criteria, 12,784 independent SNPs (i.e., one SNP
 281 randomly selected per locus) in *P. simonsi* ($n = 17$) and 13,971 independent SNPs in *P. steerei* ($n = 19$) were retained (Table
 282 S1.5). Note that fewer than the original 20 individuals per species were retained because of poor sequencing (i.e., sequences
 283 for the individual did not pass quality control filters).

284

285 **3.1. Genetic structure and genetic diversity**

286 Geographic structuring of genetic variation differs between the sympatric species, with stronger genetic structure apparent
 287 in *P. steerei* compared with *P. simonsi*. For example, *P. simonsi* individuals are scattered throughout the multivariate space
 288 (the first two PC explained 24.89% of the variance; Fig. 2a); only samples from Lower Juruá River and Purus River are
 289 relatively isolated. For *P. steerei*, three well-defined genetic clusters are clear in the multivariate space (the first two PCs
 290 explaining 46.1% of variation; Fig. 2b). Only one significant PC in *P. simonsi*, versus three significant PCs in *P. steerei*,
 291 was recognized by the Tracy-Widom tests of eigenvalues (Table S1.6). These results are consistent with sNMF (Fig. 2c) and
 292 DAPC analyses (Fig. S3.3). Namely, there is not widespread mixed ancestry among individuals of *P. steerei*; only three
 293 individuals have an ancestry with more than 20% of their genetic makeup tracing to a different cluster (Fig. 2c). This is
 294 corroborated by fairly high F_{ST} -values among the genetic clusters of *P. steerei* that range from 0.27 to 0.56 (see Table S1.7).

295 Genetic diversity is fairly similar between the species, although *P. steerei* shows higher average F_{IS} (Table S1.8),
 296 which is not surprising given the regional genetic clusters detected in *P. steerei* (Fig. 2b). In fact, there are greater
 297 differences in genetic diversity among the genetic clusters within *P. steerei* than there are between the two species (Table
 298 S1.9; Fig. S3.4).

299

300 **3.2. Isolation by Distance models**

301 Significant isolation by distance (IBD) was detected in both species using the Procrustes analyses and the Mantel tests with
 302 geographic distance, and in *P. steerei* (the seasonal floodplain species) the Mantel test based on the river network distance
 303 was also significant (Table S1.10). These results were generally robust to sequential exclusion of a genetic clusters (GCs)
 304 (in fact, the correlation coefficient increased in most of these permutations); the exception was a marginal non-significant
 305 Mantel tests based on the river network distance when GC3 in *P. steerei* was removed (Table S1.10). ANCOVA did not
 306 show significant differences in the slope of genetic and geographic distances between the species ($F = 2.179$; p -value =
 307 0.071) (Fig. S3.5a), indicating no significant differences between the species in attenuation of gene flow with geographic
 308 distance. However, the ANCOVA indicated significant differences between the species ($F = 9.2682$; p -value < 0.001; Fig.
 309 S3.5c) for Mantel tests based on river network distance along the rivers, although the slopes for the individual genetic
 310 clusters in *P. steerei* did not differ significantly (Fig. S3.5b, d).

311 The strength of the association between genes and geography as measured by the Procrustes analyses is similar
 312 between the species ($t_0 = 0.799$ for *P. simonsi* and $t_0 = 0.765$ for *P. steerei*, $p < 0.001$; Table S1.10); permutation tests show
 313 that the Procrustes results are robust (i.e., they did not change significantly when a genetic cluster was excluded; Table
 314 S1.11). However, despite similar degrees of association between genes and geography of the species, the deviations from
 315 expectations under IDB in each species, and/or the degree of deviation (even for shared localities), are not the same (Fig. 3).

316 For example, individuals from the Lower Juruá are displaced in the geo-genetic map in both species, but individuals of *P.*
 317 *simonsi* are genetically more similar to those from the Purus River region to the east, whereas the individuals of *P. steerei*
 318 are genetically more similar to those from the more southern and western Central Juruá (Fig. 3). Likewise, *P. simonsi*
 319 individuals from the Madeira are genetically more similar to those from the Central Juruá, rather than the Purus River
 320 region as in *P. steerei*. In general, individuals from the Upper Juruá and Madre de Dios in both species are positioned more
 321 similarly (Fig. 3), irrespective of whether the Galvez individuals are included.

322

323 **3.2. Isolation by Resistance models based on different environmental predictors**

324 The best IBR models in *P. simonsi* and *P. steerei* differ (Table 1; Table S1.12-S1.13) and there is no strong
 325 spatial dependence of residuals in the models for either species (Fig. S3.6). In *P. simonsi* four best fit models with $\Delta AIC < 2$
 326 recover three important predictor variables for gene flow: habitat resistance, habitat productivity, and river network
 327 distances (Fig. 4a; Table 1; Table S1.14). With a lack of significant differences among the four models (based on
 328 likelihood-ratio tests), the simplest and best fit IBR model (i.e., the one with the fewest variables) is the one with habitat
 329 resistance distance (Fig. 4b; Table S1.14), explaining around 34.9% of genetic variance (Conditional R^2 ; Table 1).
 330 Furthermore, the significance of predictors estimated by chi-squared also recovers only the habitat resistance distance as
 331 significant in each of the four models with $\Delta AIC < 2$ (Table 1), corroborating that among the five resistance predictors,
 332 habitat resistance is the only one significantly affecting functional connectivity in *P. simonsi* (i.e., higher habitat resistance
 333 distances is associated with lower relatedness of individuals, or conversely increasing the genetic distance; Fig. 4c). In *P.*
 334 *steerei* the IBR analyses recover one best fit model (with $\Delta AIC < 2$) with two important predictors: habitat resistance and
 335 the river network distance (Fig. 4d; Table 1; Table S1.14). For *P. steerei* only one model has a $\Delta AIC < 2$ and it contains two
 336 predictors that the chi-squared tests identify as significant: habitat resistance and river network distances (Fig. 4e; Table
 337 S1.14), explaining 66.8% of the genetic variance (Conditional R^2 ; Table 1). The effects of the predictor variables on
 338 functional connectivity is similar, with larger distances associated with greater genetic distances (i.e., lower values of
 339 relatedness; Fig. 4f,g).

340 For both species habitat resistance distance has a significant effect on connectivity. Although the relative
 341 importance of this variable differs between the best fit models for each species, where it is more relevant for *P. simonsi* than
 342 *P. steerei* (i.e., R^2 ; Table S1.15), the effect is similar when summed across models in each species (see Fig. 4).
 343 Topographic and Euclidean (Geographic) distances are not identified as having an important effect on functional
 344 connectivity in either species (see Fig 4; Table S1.14-S1.15).

345

346

347 **4. DISCUSSION**

348 The vast Amazon is well recognized for its incredible species richness – what is less clear is the extent to which species
 349 divergence processes follow similar routes or not. For example, not only does the heterogeneity of a landscape differ
 350 depending on the specific forest type, but differences in ecological specialization of constituent taxa are also likely to
 351 impose different constraints on gene flow. Indeed, our findings suggest that population connectivity differs between two co-
 352 distributed spiny rat species. Moreover, genetic analyses do not support the hypothesis that the seasonal floodplain *várzea*
 353 forests favor higher connectivity among populations compared to the non-flooded *terra-firme* forests. Specifically, *P.*
 354 *steerei* from the *várzea* forests shows stronger genetic structure, higher heterozygosity and lower inbreeding than *P. simonsi*

355 from the *terra-firme* forests (Fig. 2; Table S1.8). Model comparisons identifying landscape features that affect functional
 356 connectivity (i.e., the dispersal capacity) in each species showed that different forest types can impose different constraints
 357 on gene flow. We discuss evidence from our statistical modeling of genetic variation that points to factors contributing to
 358 differences in the genetic structure of the ecologically divergent sympatric taxa. As with broad generalizations about
 359 Amazonian rivers acting as barriers (see Pirani et al., 2019; Smith et al., 2014), our findings suggest that such broad
 360 generalizations about gene flow in species based on their association with specific forest types may be limited as well.

361

362 4.1. Gene flow across vast geographic areas

363 For species with distributions that cover vast areas, such as the Western Amazon, the expansive distances
 364 involved are themselves expected to influence gene flow. That is, populations separated by large geographic distances are
 365 expected to experience little gene flow compared with geographic proximate ones. Unsurprisingly, this basic expectation of
 366 isolation-by-distance (IBD) is met in both spiny rate species. Geographic distance also explains similar proportions of
 367 genetic variation between the sympatric species (i.e., the strength of the relationship between geographic and genetic
 368 distance is similar; see Fig. 3, Fig. S3.5, and Table S1.10), and there is no significant difference in the attenuation of gene
 369 flow with Euclidean geographic distance between the species (Fig. S3.5). Note that the similar fits to IBD models are
 370 unlikely to be an artifact of population size disparities (see Excoffier et al., 2009; but see He et al., 2013), suggesting that
 371 connectivity does not differ between the species. However, this similarity in the fits of IBD models might reflect the
 372 geographical scale of the study. At large spatial scales of broadly distributed species, the potential effects of habitat
 373 association on connectivity may be masked by the predominant effects of geographic distance (Lanier et al., 2015; Massatti
 374 & Knowles, 2014).

375 Despite their fit to IBD, the species show some pronounced differences in their respective deviations from IBD
 376 and geographic structuring of genetic variation (Fig. 2). For example, the deviations from IBD evident in geo-genetic space
 377 of the Procrustes analysis (Fig. 3) in the seasonal floodplain species, *P. steerei*, follow the river channel in the genetic
 378 cluster (GC) 1 and GC3, while the deviations in GC2 is restricted to headwaters areas (Fig. 3b). This result is consistent
 379 with the significant IBD Mantel tests based on river network distance (Table S1.10; Fig. S3.5c), as with tests in other
 380 aquatic species (e.g., Murphy et al., 2018).

381 These results reinforce the impact of rivers on gene flow. However, in the Western Amazon (and at least for the
 382 taxa studied here) an argument can be made for a more nuanced perspective, and one that recognizes that when rivers act as
 383 conduits for gene flow, the lack of river connections can leave an indelible mark on genetic variation in floodplain *várzea*
 384 forest inhabitants (Fig. 3). In our study, a factor limiting gene flow may be the restricted distribution of seasonal floodplain
 385 forest at headwaters (Salo et al., 1986; Hess et al., 2015). Specifically, if the lack of rivers routes for dispersal in *P. steerei*
 386 results in regional structuring of genetic variation (Fig. 3b), but only in this floodplain *várzea* forest taxon that utilizes rivers
 387 for dispersal, then the absence of region genetic structuring in *P. simonsi* (Fig. 3a) is less surprising. However, if rivers were
 388 acting as barriers (e.g., Ribas et al., 2012), the difference in regional structuring would remain an unresolved conundrum
 389 because it seems very unlikely that *P. simonsi*'s association with non-flooded *terra-firme* forest would make it less prone to
 390 be influenced by historical barriers associated with rivers.

391 On the surface, this perspective might seem to be contradictory with existing literature. For example, we note that
 392 the pronounced regional structuring of genetic variation detected in *P. steerei* is similar to expectations based on the effects
 393 of historical barriers in other Amazonian regions (e.g., Da Silva & Patton, 1998 Fernandes et al., 2013). The genetic clusters

394 detected in *P. steerei* (Fig. 2), and specifically the delineation of genetic cluster 2 and 3 (GC2 and GC3 in Fig. 3) indeed
 395 coincide with the Iquitos structural arch, a geomorphological feature that demarcates geological units associated with the
 396 origin of river basins and subbasins in the Amazon (Albert et al., 2018). However, this correspondence between genetic
 397 divergence patterns with the formation of geographic barriers (e.g., the Iquitos Arch, which blocked the transport of
 398 Andean-derived sediments from the Western Amazon during the Pliocene; van Soelen et al., 2017), which has been
 399 identified in other phylogeographic studies of vertebrates in the region (e.g., Da Silva & Patton, 1998; Gascon et al., 2000;
 400 Patton et al., 2000). Our work highlights that this correspondence should not be reflexively viewed as evidence of the river
 401 barrier hypothesis, and that it is also entirely consistent with the hypothesis of a lack of river connections, especially in
 402 species in which rivers serve as routes of dispersal (i.e., in floodplain *várzea* forest inhabitants, but not those from the *terra-*
 403 *firme* forests).

404 As discussed below, with 46.7% in *P. simonsi* and 59.9% in *P. steerei* of genetic variance explained by the best
 405 fit IBR models (i.e., upper bound for conditional R^2 ; Table 1), a considerable amount of variation remains unexplained by
 406 the IBR models. This indicates that there are factors that were not explicitly tested in our study. It is possible that the
 407 association between gene and geography on a regional scale relates to variation in the historical stability of the South
 408 American wetlands (Prado et al., 2019). However, studies have shown little variation in precipitation (Cheng et al., 2013),
 409 temperature (Colinvaux et al., 1996), and vegetation (Häggi et al., 2017) since the last glacial maximum (Pleistocene) in the
 410 Western Amazon. Previous mtDNA genetic studies have also suggested stable population sizes in both *P. steerei* and *P.*
 411 *simonsi* in the Western Amazon since the last glacial maximum (Lessa et al., 2003; Matocq et al., 2000). So, it seems
 412 unlikely stability is responsible for the differences in regional structuring of genetic variation between the spiny rat species.
 413 Dissecting the association between genes and geography further, shows that there are also some differences between the
 414 species in the structure of genetic variation locally (for example, individuals from the Lower Juruá and Purus in both
 415 species; Fig. 3). However, additional taxa are needed to evaluate the extent to which there might be a deterministic
 416 explanation, and to rule out the possibility that some of the differences reflect historical contingency.

417

418 **4.2 Forest association and functional connectivity in spiny rats**

419 Tests of the suite of models for explaining functional connectivity in *P. steerei* and *P. simonsi* as a function of
 420 various ecological and environmental predictor variables share some common features. All variables representing
 421 differences between forest types (habitat resistance, habitat productivity, and river network distance) were detected as
 422 important influence on functional connectivity in at least one of the species (Fig 4; for details see Table S1.15); the primary
 423 exception is topographic distance, which may simply reflect the relative lack of variation in altitude in Western Amazon at
 424 the scale of our study (Vormisto et al., 2004). Moreover, in neither species is the effect of geographic distance (while
 425 significant in the Mantel tests) a component of the best fit IBR models that incorporate environmental variables (Table 1),
 426 nor does it have a significant contribution when summing across IBR models (Fig. 4). This difference in the effect of
 427 geographic distance is not unexpected because resistance variables that co-vary with geographic distance may lead to
 428 spurious inferences (Dormann et al., 2013; Fig. S3.2), and the MLPE mixed models account for the non-independence of
 429 genetic pairwise distances variables, unlike Mantel tests, which can inflate r^2 values (Clark et al., 2002; Harrison et al. 2018;
 430 Shirk et al., 2018; Silk et al. 2020).

431 With respect to the best fit or most probable models in predicting genetic variation, there was one key variable in
 432 common to both species: habitat resistance (river network distances were present only in *P. steerei*; Table 1). This variable

433 corroborates the potential links to mechanistic or functional predictors of gene flow for taxa with different forest
 434 associations; the variable habitat resistance also explains more than three times the genetic variance in *P. simonsi* species,
 435 the non-flooded (*terra-firme*) species, than in *P. steerei* (R_s^2 in Table S1.15). Habitat resistance and river network capture
 436 different aspects of the ease of dispersal (i.e., resistance), across the landscape (see Appendix S2.2 for details on quantifying
 437 resistance for these two variables), and thus presumably gene flow across the landscape. Specifically, habitat resistance
 438 distance captures the relative likelihood of gene flow between sampled sites as a function of the distribution of wetland
 439 versus non-wetland habitats between those sites (i.e., traversing wetlands will not impose much resistance to gene flow for
 440 *P. steerei*, which inhabits the seasonal floodplain *várzea* forests, but wetlands would impose high resistance to gene flow in
 441 *P. simonsi*, which inhabits non-flooded *terra-firme* forest). In a similar fashion, connectivity via rivers is expected for *P.*
 442 *steerei*, which inhabits the seasonal floodplain forests distributed along rivers. If gene flow among sampled sites of *P.*
 443 *steerei* is primarily via river routes (as supported by Mantel tests – Table S1.10 and IBR models – Fig. 4), this could explain
 444 the small but significant contribution of the habitat resistance distance variable to functional connectivity in the species
 445 (Table S1.15). Furthermore, during the annual inundations, the seasonal floodplain species *P. steerei* can occupy higher
 446 areas in the *várzea* forests or can move to adjacent non-flooded *terra-firme* areas, while *P. simonsi* the *terra-firme* species
 447 remains in its habitat given lack of evidence for movement across different forest types (see Matocq et al., 2000; Patton &
 448 Leite, 2015). As such, the relative importance of different environmental variables, especially habitat resistance, in
 449 predicting function connectivity in *P. steerei* versus *P. simonsi* also suggests that species-specific traits, in this case specific
 450 forest associations, can determine functional connectivity across populations. That is, dispersal in spiny rat taxa, and
 451 specifically those associated with floodplain *várzea* forest (but not *terra-firme* forests) maybe facilitated by rivers.

452 Studies of additional taxa, especially other mammal species, will provide the context to discern whether the spiny
 453 rat taxa studied here are atypical, or that differences in the traits of mammals compared with birds and plants underlie
 454 differing support for hypothesized connectivity based on forest-type (Papadopoulou & Knowles, 2016). We also recognize
 455 that our results are in contrast with some aspects of mtDNA study of *P. steerei* and *P. simonsi* from the Juruá River (see
 456 Matocq et al., 2000). Differences in the geographic scale of our study no doubt contributes to the differences observed
 457 between genomic variation and mtDNA variation (i.e., our results are based on analyses of individuals across the species’
 458 ranges, which span multiple rivers).

459 Our statistical modeling and fit of the data to different models points to specific environmental and habitat
 460 differences between the ecological divergent spiny rat species that may contribute to differences in the genetic structure of
 461 these sympatric taxa. Specifically, wetland habitats inhibit and promote the functional connectivity in *P. simonsi* and *P.*
 462 *steerei*, respectively, although large distances along the rivers can prevent gene flow in both taxa (i.e., gene flow attenuates
 463 with geographic distance). Despite the significance of environmental and habitat variables associated with floodplain *várzea*
 464 forests versus non-flooded *terra-firme* forest that explain the genetic variation in the two taxa, it is notable that connectivity
 465 is not higher in the floodplain *várzea* forest species *P. steerei* as posited by traditional hypotheses and supported in bird
 466 species (Aleixo, 2006; Cadena et al., 2011; Harvey et al., 2017; but see Thom et al., 2020) and in some plants (Godoy et al.,
 467 1999). Furthermore, a significant proportion of unexplained genetic variance in the spiny rats indicates that differences in
 468 connectivity between the taxa cannot be understood through the lens of a single dimension of Amazonian heterogeneity –
 469 that is, forest type. In fact, we develop the argument that the presence of regional geographic structuring in *P. steerei* that is
 470 absent in *P. simonsi*, suggests that the lack of river connections, as well as other unidentified factors, play an important role
 471 in restricting gene flow.

472 Irrespective of the combination of factors that best explains genetic variation in the spiny rats *P. steerei* or *P.*
473 *simonsi*, our study does raise questions about the spectre of generalizable predictions about connectivity in species
474 associated with seasonal floodplain *várzea* forests versus non-flooded *terra-firme* forest. As with other generalities that have
475 been put forth for processes of divergence in the Amazon (e.g., the proposition that the major Amazon rivers act as barriers;
476 see Pirani et al., 2019), generalized expectations for the divergence process in species that inhabit different forest types may
477 similarly be limited in their explanatory power. Given the incredible biodiversity that characterizes the Amazon, perhaps it
478 should not be expected that this diversity will follow a common set of predictions for genetic structure, or conversely
479 connectivity, or surprising when it doesn't.

480 **Tables**

481 **Table 1:** The best fit models ($\Delta\text{AIC} < 2$ with the best fit model in bold) for observed geographic distribution of relatedness coefficients in *P. simonsi* (the non-flooded
 482 forest/*terra-firme* species) and in *P. steerei*, (the seasonal floodplain forests/*várzea* species) using MLPE. The contribution of each predictor variable (and standard error,
 483 in parentheses) calculated with REML (see Material and Methods for details) are shown, as the significance of chi-squared contingency table tests each predictor in the
 484 models, with * for $p < 0.05$, ** for $p < 0.01$, ^{ns} if not significant. There was no statistically significant difference in the fit of the best models (in bold) for *P. simonsi*
 485 species and the other models using the likelihood-ratio tests (LRT) in p -value column. Log-likelihoods (logL), and correlation coefficient, ρ , between relatedness
 486 coefficients and distances specified by each model. The conditional R^2 and its confidence intervals in parenthesis (a measure of variance explained by the entire model,
 487 including fixed and random effects) are also shown for the best fit models. Results for all models taking into account the correlations among the predictors variables (i.e.,
 488 the uncorrelated models) are presented in Tables S1.12-S1.13.

489

Models	Habitat	Productivity	River	logL	ρ	Conditional R^2 (C.I. 95%)	p -value
<i>P. simonsi</i> :							
Habitat** + Productivity ^{ns}	-0.091 (0.015)	-0.020 (0.017)	.	58.698	0.048		0.149
Habitat**	-0.098 (0.013)	.	.	60.767	0.028	0.349 (0.233 – 0.467)	.
Habitat** + River ^{ns}	-0.095 (0.015)	.	-0.008 (0.015)	57.568	0.026		0.597
Habitat** + Productivity ^{ns} + River ^{ns}	-0.092 (0.016)	-0.021 (0.019)	0.003 (0.016)	55.577	0.050		0.345
<i>P. steerei</i> :							
Habitat** + River**	-0.032 (0.006)	.	-0.111 (0.008)	163.332	0.469	0.668 (0.732 – 0.599)	.

490

491

492

493 **FIGURE LEGENDS**

494 **Figure 1.** Geographical sampling of individuals for the genomics analyses of two sympatric *Proechimys* species from the
 495 Western Amazon, which differ in their habitat associations, with *P. simonsi* (shown in squares) in the non-flooded forests
 496 (*terra-firme*), and *P. steerei* (shown in triangles) in the seasonal floodplain forests (*várzea*). Each sample locality is color-
 497 coded according to regional Amazonian rivers (see labels); gray areas represent known distribution range for these species,
 498 according to IUCN (www.iucnredlist.org) with pointed line for *P. simonsi* and dashed line for *P. steerei*; forested areas are
 499 shown in green and open areas in beige; map inset shows area of study.

500

501 **Figure 2.** Principal Components Analysis (PCA) of (a) *P. simonsi* (non-flooded forests/*terra-firme*, as represented by the
 502 icon) and (b) *P. steerei* (seasonal floodplain forests/*várzea*, as represented by the icon), with individuals color-coded by the
 503 different river regions (see Fig. 1 for distribution details). The three genetic clusters (GC) delineated in *P. steerei* were also
 504 identified by (c) the sNMF approach based on ancestry coefficients, whereas a single genetic cluster was identified for *P.*
 505 *simonsi* (see Fig. S3.3).

506

507 **Figure 3.** Procrustes analyses of (a) *P. simonsi* and (b) *P. steerei* with triangles representing the geographical sampling
 508 localities and circles the individuals in geo-genetic space (symbols are color-coded by the different river regions). The
 509 length of the lines connecting the individuals to their respective sample localities (i.e., circles to the triangles) represent the
 510 degree of the deviation from the expectation in geo-genetic space under an isolation by distance model, with longer lines
 511 representing greater deviations. The three genetic clusters in *P. steerei* (see also Fig. 2) are labeled and demarcated by
 512 dotted lines. Forested areas are shown in green on the map and open areas in beige; map inset shows area of study. Icons for
 513 the non-flooded forests/*terra-firme* in plot a, and the seasonal floodplain forests/*várzea* in plot b are shown.

514

515 **Figure 4.** Relative importance of each environmental predictor variable in explaining functional connectivity for the best fit
 516 models ($\Delta AIC < 2$) among the MLPE regression models for (a) *P. simonsi* and (d) *P. steerei* are shown in blue, where the
 517 relative importance of a variable increases towards the outer edge of the circle (circular dashed lines represent 0%, 50% and
 518 100% of importance from the innermost to the outermost line, respectively). Importance values are based on the sum of AIC
 519 weights over all models that include the predictor variable (for details see Table S1.15). Also shown are the icons for the
 520 non-flooded forests/*terra-firme* in plot a, and the seasonal floodplain forests/*várzea* in plot d. Coefficient plots for best-
 521 fitting models ($\Delta AIC \leq 2$) for (b) *P. simonsi* and (e) *P. steerei* (see Table S1.14 for details). Points represent model-
 522 averaged regression coefficients and horizontal lines the 95% confidence intervals. Variables that do not touch the vertical
 523 dashed line (0.00) are considered significant for models similarly to LTR results. Isolation-by-resistance effects of
 524 significant variables in (c) *P. simonsi* and (f-g) *P. steerei*. Plots indicate relationship between the relatedness coefficient
 525 (REL) and habitat resistance in (c) *P. simonsi* and in (f) *P. steerei* and river distance in (g) *P. steerei*. Relatedness values are
 526 decorrelated for the MLPE correlation structure.

527

528 **DATA AVAILABILITY STATEMENT**

529 Genetic data and Supporting Information are available in Dryad: <https://doi.org/10.5061/dryad.4qrfj6qbf>

530 All R scripts are available at: https://github.com/jdalapicolla/LanGen_pipeline_version2;

531 https://github.com/jdalapicolla/IBD_models.R; <https://github.com/jdalapicolla/MLPE.R>

532 REFERENCES

- 533 Albert, J. S., Val, P., Hoorn, C., Albert, J. S., Val, P., & Hoorn, C. (2018). The changing course of the Amazon River in the Neogene: center stage for
534 Neotropical diversification. *Neotropical Ichthyology*, *16*(3), e180033. <https://doi.org/10.1590/1982-0224-20180033>
- 535 Aleixo, A. (2006). Historical diversification of floodplain forest specialist species in the Amazon: a case study with two species of the avian genus
536 *Xiphorhynchus* (Aves: Dendrocolaptidae). *Biological Journal of the Linnean Society*, *89*(2), 383–395. <https://doi.org/10.1111/j.1095-8312.2006.00703.x>
- 538 Balkenhol, N., Cushman, S., Storf, A., & Waits, L. (2015). *Landscape genetics: concepts, methods, applications*. John Wiley & Sons.
- 539 Barlow, J., Lennox, G. D., Ferreira, J., Berenguer, E., Lees, A. C., Nally, R., ... Gardner, T. A. (2016). Anthropogenic disturbance in tropical forests can
540 double biodiversity loss from deforestation. *Nature*, *535*(7610), 144–147. <https://doi.org/10.1038/nature18326>
- 541 Bredin, Y. K., Hawes, J. E., Peres, C. A., & Hugaasen, T. (2020). Structure and composition of terra firme and seasonally flooded várzea forests in the
542 western Brazilian Amazon. *Forests*, *11*(12), 1–20. <https://doi.org/10.3390/f11121361>
- 543 Cadena, C. D., Gutiérrez-Pinto, N., Dávila, N., & Terry Chesser, R. (2011). No population genetic structure in a widespread aquatic songbird from the
544 Neotropics. *Molecular Phylogenetics and Evolution*, *58*(3), 540–545. <https://doi.org/10.1016/j.ympev.2010.12.014>
- 545 Carnaval, A. C., & Moritz, C. (2008). Historical climate modelling predicts patterns of current biodiversity in the Brazilian Atlantic forest. *Journal of*
546 *Biogeography*, *35*(7), 1187–1201. <https://doi.org/10.1111/j.1365-2699.2007.01870.x>
- 547 Carvalho, C. S., Lanes, É. C. M., Silva, A. R., Caldeira, C. F., Carvalho-Filho, N., Gastauer, M., Imperatriz-Fonseca, V. L., Nascimento Júnior, W.,
548 Oliveira, G., Siqueira, J. O., Viana, P. L., & Jaffé, R. (2019). Habitat loss does not always entail negative genetic consequences. *Frontiers in*
549 *Genetics*, *10*, 1101. <https://doi.org/10.3389/fgene.2019.01101>
- 550 Castilla, A. R., Méndez-Vigo, B., Marcer, A., Martínez-Minaya, J., Conesa, D., Picó, F. X., & Alonso-Blanco, C. (2020). Ecological, genetic and
551 evolutionary drivers of regional genetic differentiation in *Arabidopsis thaliana*. *BMC Evolutionary Biology*, *20*(1), 1–13.
552 <https://doi.org/https://doi.org/10.1186/s12862-020-01635-2>
- 553 Cheng, H., Sinha, A., Cruz, F. W., Wang, X., Edwards, R. L., d'Horta, F. M., Ribas, C. C., Vuille, M., Stott, L. D., & Auler, A. S. (2013). Climate change
554 patterns in Amazonia and biodiversity. *Nature Communications*, *4*(1), 1411. <https://doi.org/10.1038/ncomms2415>
- 555 Clarke, R. T., Rothery, P., & Raybould, A. F. (2002). Confidence limits for regression relationships between distance matrices: Estimating gene flow with
556 distance. *Journal of Agricultural, Biological, and Environmental Statistics*, *7*(3), 361–372. <https://doi.org/10.1198/108571102320>
- 557 Colinvaux, P. A., De Oliveira, P. E., Moreno, J. E., Miller, M. C., & Bush, M. B. (1996). A long pollen record from lowland Amazonia: forest and cooling
558 in glacial times. *Science*, *274*(5284), 85–88. <https://doi.org/10.1126/science.274.5284.85>
- 559 Constantine, J. A., Dunne, T., Ahmed, J., Legleiter, C., & Lazarus, E. D. (2014). Sediment supply as a driver of river meandering and floodplain evolution
560 in the Amazon Basin. *Nature Geoscience*, *7*(12), 899–903. <https://doi.org/10.1038/ngeo2282>
- 561 Dalapicolla, J., Alves, R., Jaffé, R., Vasconcelos, S., Pires, E. S., Nunes, G. L., ... Oliveira, G. (2021). Conservation implications of genetic structure in the
562 narrowest endemic quillwort from the Eastern Amazon. *Ecology and Evolution*, *11*(15), 10119–10132. <https://doi.org/10.1002/ECE3.7812>
- 563 Da Silva, M. N., & Patton, J. L. (1998). Molecular phylogeography and the evolution and conservation of amazonian mammals. *Molecular Ecology*, *7*,
564 475–486. <https://doi.org/10.1046/j.1365-294x.1998.00276.x>
- 565 Dormann, C. F., Elith, J., Bacher, S., Buchmann, C., Carl, G., Carré, G., ... Lautenbach, S. (2013). Collinearity: a review of methods to deal with it and a
566 simulation study evaluating their performance. *Ecography*, *36*(1), 27–46. <https://doi.org/10.1111/j.1600-0587.2012.07348.x>
- 567 Dray, S., & Dufour, A. B. (2007). The ade4 package: implementing the duality diagram for ecologists. *Journal of Statistical Software*, *22*(4), 1–20.
568 <https://doi.org/10.18637/jss.v022.i04>
- 569 Emmons, L. H. (1982). Ecology of *Proechimys* (Rodentia, Echimyidae) in southeastern Peru. *Tropical Ecology*, *23*(2), 280–290.
- 570 Excoffier, L., Foll, M., & Petit, R. J. (2009). Genetic consequences of range expansions. *Annual Review of Ecology, Evolution, and Systematics*, *40*(1),
571 481–501. <https://doi.org/10.1146/annurev.ecolsys.39.110707.173414>
- 572 Fabre, P. H., Patton, J. L., & Leite, Y. L. R. (2016). Family Echimyidae (hutias, South American spiny-rats and coypu). In D. E. Wilson, T. E. J. Lacher, &
573 R. A. Mittermeier (Eds.), *Handbook of the Mammals of the World. Vol 6. Lagomorphs and Rodents I* (pp. 552–641). Lynx Edicions.
- 574 Fenderson, L. E., Kovach, A. I., & Llamas, B. (2020). Spatiotemporal landscape genetics: Investigating ecology and evolution through space and time.
575 *Molecular Ecology*, *29*(2), 218–246. <https://doi.org/10.1111/mec.15315>
- 576 Fernandes, A. M., Gonzalez, J., Wink, M., & Aleixo, A. (2013). Multilocus phylogeography of the Wedge-billed Woodcreeper *Glyphorhynchus spirurus*
577 (Aves, Furnariidae) in lowland Amazonia: widespread cryptic diversity and paraphyly reveal a complex diversification pattern. *Molecular*
578 *Phylogenetics and Evolution*, *66*(1), 270–282. <https://doi.org/10.1016/j.ympev.2012.09.033>
- 579 Fricot, E., & Francois, O. (2014). *LEA: an R package for landscape and ecological association studies*. [http://membres-](http://membres-timc.imag.fr/Olivier.Francois/lea.html)
580 [timc.imag.fr/Olivier.Francois/lea.html](http://membres-timc.imag.fr/Olivier.Francois/lea.html)

- 581 Frichot, E., Mathieu, F., Trouillon, T., Bouchard, G., & François, O. (2014). Fast and efficient estimation of individual ancestry coefficients. *Genetics*,
582 196(4), 973–983. <https://doi.org/10.1534/genetics.113.160572>
- 583 Gascon, C., Malcolm, J. R., Patton, J. L., da Silva, M. N., Bogart, J. P., Lougheed, S. C., ... Boag, P. T. (2000). Riverine barriers and the geographic
584 distribution of Amazonian species. *Proceedings of the National Academy of Sciences*, 97(25), 13672–13677.
585 <https://doi.org/10.1073/pnas.230136397>
- 586 Godoy, J. R., Petts, G., & Salo, J. (1999). Riparian flooded forests of the Orinoco and Amazon basins: A comparative review. *Biodiversity and
587 Conservation*, 8(4), 551–586. <https://doi.org/10.1023/A:1008846531941>
- 588 Goslee, S. C., & Urban, D. L. (2007). The ecodist package for dissimilarity-based analysis of ecological data. *Journal of Statistical Software*, 22(7), 1–19.
589 <https://doi.org/10.18637/jss.v022.i07>
- 590 Gruber, B., & Georges, A. (2019). *dartR: importing and analysing SNP and silicodart data generated by genome-wide restriction fragment analysis*.
591 <https://cran.r-project.org/package=dartR>
- 592 Gumbrecht, T., Roman-Cuesta, R. M., Verchot, L., Herold, M., Wittmann, F., Householder, E., ... Murdiyarsa, D. (2017). An expert system model for
593 mapping tropical wetlands and peatlands reveals South America as the largest contributor. *Global Change Biology*, 23(9), 3581–3599.
594 <https://doi.org/10.1111/gcb.13689>
- 595 Häggi, C., Chiessi, C. M., Merkel, U., Multiza, S., Prange, M., Schulz, M., & Schefuß, E. (2017). Response of the Amazon rainforest to late Pleistocene
596 climate variability. *Earth and Planetary Science Letters*, 479, 50–59. <https://doi.org/10.1016/J.EPSL.2017.09.013>
- 597 Harrison, X. A., Donaldson, L., Correa-Cano, M. E., Evans, J., Fisher, D. N., Goodwin, C. E. D., Robinson, B. S., Hodgson, D. J., & Inger, R. (2018). A
598 brief introduction to mixed effects modelling and multi-model inference in ecology. *PeerJ*, 2018(5), e4794. <https://doi.org/10.7717/peerj.4794>
- 599 Harvey, M. G., Aleixo, A., Ribas, C. C., & Brumfield, R. T. (2017). Habitat association predicts genetic diversity and population divergence in amazonian
600 birds. *American Naturalist*, 190(5), 631–648. <https://doi.org/10.1086/693856>
- 601 Hawkins, B. A., Porter, E. E., & Diniz-Filho, J. A. F. (2003). Productivity and history as predictors of the latitudinal diversity gradient of terrestrial birds.
602 *Ecology*, 84(6), 1608–1623. [https://doi.org/10.1890/0012-9658\(2003\)084\[1608:PAHAPO\]2.0.CO;2](https://doi.org/10.1890/0012-9658(2003)084[1608:PAHAPO]2.0.CO;2)
- 603 He, Q., Edwards, D. L., & Knowles, L. L. (2013). Integrative testing of how environments from the past to the present shape genetic structure across
604 landscapes. *Evolution*, 67(12), 3386–3402. <https://doi.org/10.1111/evo.12159>
- 605 Hess, L. L., Melack, J. M., Affonso, A. G., Barbosa, C., Gastil-Buhl, M., & Novo, E. M. L. M. (2015). Wetlands of the Lowland Amazon Basin: Extent,
606 Vegetative Cover, and Dual-season Inundated Area as Mapped with JERS-1 Synthetic Aperture Radar. *Wetlands*, 35(4), 745–756.
607 <https://doi.org/10.1007/s13157-015-0666-y>
- 608 Hijmans, R., & van Etten, J. (2015). raster: Geographic Data Analysis and Modeling. In *R package version 3.4-10*.
- 609 Hoban, S., Bruford, M., D'Urban Jackson, J., Lopes-Fernandes, M., Heuertz, M., Hohenlohe, P. A., ... Laikre, L. (2020). Genetic diversity targets and
610 indicators in the CBD post-2020 Global Biodiversity Framework must be improved. *Biological Conservation*, 248, 108654.
611 <https://doi.org/10.1016/j.biocon.2020.108654>
- 612 Hoorn, C., Wesselingh, F. P., ter Steege, H., Bermudez, M. A., Mora, A., Sevink, J., ... Antonelli, A. (2010). Amazonia through time: Andean uplift,
613 climate change, landscape evolution, and biodiversity. *Science*, 330(6006), 927–931. <https://doi.org/10.1126/science.1194585>
- 614 Jaeger, B. C. (2017). *r2glmm: computes R squared for mixed (multilevel) models*. <https://cran.r-project.org/package=r2glmm>
- 615 Jaeger, B. C., Edwards, L. J., Das, K., & Sen, P. K. (2017). An R2 statistic for fixed effects in the generalized linear mixed model. *Journal of Applied
616 Statistics*, 44(6), 1086–1105. <https://doi.org/10.1080/02664763.2016.1193725>
- 617 Jaffé, R., Veiga, J. C., Pope, N. S., Lanes, É. C. M., Carvalho, C. S., Alves, R., ... Imperatriz-Fonseca, V. L. (2019). Landscape genomics to the rescue of a
618 tropical bee threatened by habitat loss and climate change. *Evolutionary Applications*, 12(6), 1164–1177. <https://doi.org/10.1111/eva.12794>
- 619 Jombart, T., & Ahmed, I. (2011). adegenet 1.3-1: new tools for the analysis of genome-wide SNP data. *Bioinformatics*, 27(21), 3070–3071.
620 <https://doi.org/10.1093/bioinformatics/btr521>
- 621 Jombart, T., Devillard, S., & Balloux, F. (2010). Discriminant analysis of principal components: A new method for the analysis of genetically structured
622 populations. *BMC Genetics*, 11(1), 1–15. <https://doi.org/10.1186/1471-2156-11-94>
- 623 Junk, W. J., & Piedade, M. T. (1993). Herbaceous plants of the Amazon floodplain near Manaus: Species diversity and adaptations to the flood pulse.
624 *Amazoniana: Limnologia et Oecologia Regionalis Systematis Fluminis Amazonas*, 12(3/4), 467–484. [http://hdl.handle.net/21.11116/0000-0004-
625 896E-7](http://hdl.handle.net/21.11116/0000-0004-896E-7)
- 626 Knowles, L. L., Massatti, R., He, Q., Olson, L. E., & Lanier, H. C. (2016). Quantifying the similarity between genes and geography across Alaska's alpine
627 small mammals. *Journal of Biogeography*, 43(7), 1464–1476. <https://doi.org/10.1111/jbi.12728>
- 628 Lanier, H. C., Massatti, R., He, Q., Olson, L. E., & Knowles, L. L. (2015). Colonization from divergent ancestors: glaciation signatures on contemporary
629 patterns of genomic variation in Collared Pikas (*Ochotona collaris*). *Molecular Ecology*, 24(14), 3688–3705. <https://doi.org/10.1111/mec.13270>

- 630 Lara, M., & Patton, J. L. (2000). Evolutionary diversification of spiny rats (genus *Trinomys*, Rodentia: Echimyidae) in the Atlantic Forest of Brazil.
631 *Zoological Journal of the Linnean Society*, 130(4), 661–686. <https://doi.org/10.1006/zjls.2000.0240>
- 632 Leite, R. N., & Rogers, D. S. (2013). Revisiting Amazonian phylogeography: insights into diversification hypotheses and novel perspectives. *Organisms*
633 *Diversity & Evolution*, 13(4), 639–664. <https://doi.org/10.1007/s13127-013-0140-8>
- 634 Leite, Y. L. R. (2003). Evolution and systematics of the Atlantic Tree Rats, genus *Phyllomys* (Rodentia: Echimyidae) with description of two new species.
635 *University of California Publications in Zoology*, 132, 1–118.
- 636 Lessa, E. P., Cook, J. A., & Patton, J. L. (2003). Genetic footprints of demographic expansion in North America, but not Amazonia, during the Late
637 Quaternary. *Proceedings of the National Academy of Sciences of the United States of America*, 100(18), 10331–10334.
638 <https://doi.org/10.1073/pnas.1730921100>
- 639 Li, H., Qu, W., Obrycki, J. J., Meng, L., Zhou, X., Chu, D., & Li, B. (2020). Optimizing sample size for population genomic study in a global invasive lady
640 beetle, *Harmonia axyridis*. *Insects*, 11(5), 290. <https://doi.org/10.3390/insects11050290>
- 641 Li, W., Zhang, P., Ye, J., Li, L., & Baker, P. A. (2011). Impact of two different types of El Niño events on the Amazon climate and ecosystem
642 productivity. *Journal of Plant Ecology*, 4(1–2), 91–99. <https://doi.org/10.1093/jpe/rtq039>
- 643 Manel, S., & Holderegger, R. (2013). Ten years of landscape genetics. *Trends in Ecology and Evolution*, 28(10), 614–621.
644 <https://doi.org/10.1016/j.tree.2013.05.012>
- 645 Manel, S., Schwartz, M. K., Luikart, G., & Taberlet, P. (2003). Landscape genetics: Combining landscape ecology and population genetics. *Trends in*
646 *Ecology and Evolution*, 18(4), 189–197. [https://doi.org/10.1016/S0169-5347\(03\)00008-9](https://doi.org/10.1016/S0169-5347(03)00008-9)
- 647 Mantel, N. (1967). The detection of disease clustering and a generalized regression approach. *Cancer Research*, 27(2), 209–220.
648 <http://www.ncbi.nlm.nih.gov/pubmed/6018555>
- 649 Massatti, R., & Knowles, L. L. (2014). Microhabitat differences impact phylogeographic concordance of codistributed species: genomic evidence in
650 montane sedges (*Carex* L.) from the Rocky Mountains. *Evolution*, 68(10), 2833–2846. <https://doi.org/10.1111/evo.12491>
- 651 Massatti, R., & Knowles, L. L. (2016). Contrasting support for alternative models of genomic variation based on microhabitat preference: species-specific
652 effects of climate change in alpine sedges. *Molecular Ecology*, 25(16), 3974–3986. <https://doi.org/10.1111/mec.13735>
- 653 Matocq, M. D., Patton, J. L., & Da Silva, M. N. F. (2000). Population genetic structure of two ecologically distinct amazonian spiny rats: separating history
654 and current ecology. *Evolution*, 54(4), 1423–1432. <https://doi.org/10.1111/j.0014-3820.2000.tb00574.x>
- 655 McLaughlin, J. F., & Winker, K. (2020). An empirical examination of sample size effects on population demographic estimates in birds using single
656 nucleotide polymorphism (SNP) data. *PeerJ*, 8, e9939. <https://doi.org/10.7717/peerj.9939>
- 657 McRae, B. H. (2006). Isolation by resistance. *Evolution*, 60(8), 1551–1561. <https://doi.org/10.1111/j.0014-3820.2006.tb00500.x>
- 658 McRae, B. H., & Beier, P. (2007). Circuit theory predicts gene flow in plant and animal populations. *Proc Natl Acad Sci U S A*, 104(50), 19885–19890.
659 <https://doi.org/10.1073/pnas.0706568104>
- 660 Miller, J. M., Cullingham, C. I., & Peery, R. M. (2020). The influence of a priori grouping on inference of genetic clusters: simulation study and literature
661 review of the DAPC method. *Heredity*, 125(5), 269–280. <https://doi.org/10.1038/s41437-020-0348-2>
- 662 Murphy, M. O., Jones, K. S., Price, S. J., & Weisrock, D. W. (2018). A genomic assessment of population structure and gene flow in an aquatic salamander
663 identifies the roles of spatial scale, barriers, and river architecture. *Freshwater Biology*, 63(5), 407–419. <https://doi.org/10.1111/fwb.13071>
- 664 Nakagawa, S., & Schielzeth, H. (2013). A general and simple method for obtaining R^2 from generalized linear mixed-effects models. *Methods in Ecology*
665 *and Evolution*, 4(2), 133–142. <https://doi.org/10.1111/j.2041-210x.2012.00261.x>
- 666 Nazareno, A. G., Bemmels, J. B., Dick, C. W., & Lohmann, L. G. (2017). Minimum sample sizes for population genomics: an empirical study from an
667 Amazonian plant species. *Molecular Ecology Resources*, 17(6), 1136–1147. <https://doi.org/10.1111/1755-0998.12654>
- 668 Oksanen, J., Blanchet, F. G., Friendly, M., Kindt, R., Legendre, P., O'Hara, R. B., Simpson, G. L., Solymos, P., Stevens, M. H. H., Szoecs, E., & Wagner,
669 H. (2019). *vegan: community ecology package*. <http://cran.r-project.org/package=vegan>
- 670 Papadopoulou, A., & Knowles, L. L. (2016). Toward a paradigm shift in comparative phylogeography driven by trait-based hypotheses. *Proceedings of the*
671 *National Academy of Sciences of the United States of America*, 113(29), 8018–8024. <https://doi.org/10.1073/pnas.1601069113>
- 672 Patterson, N., Price, A. L., & Reich, D. (2006). Population structure and eigenanalysis. *PLoS Genetics*, 2(12), 2074–2093.
673 <https://doi.org/10.1371/journal.pgen.0020190>
- 674 Patton, J. L., & Leite, R. N. (2015). Genus *Proechimys* J. A. Allen, 1889. In J. L. Patton, U. F. J. Pardiñas, & G. D'Elia (Eds.), *Mammals of South America*,
675 *Volume 2: Rodents* (pp. 950–989). University Of Chicago Press.
- 676 Patton, J. L., Da Silva, M. N., & Malcolm, J. R. (2000). Mammals of the rio Juruá and the evolutionary and ecological diversification of Amazonia.
677 *Bulletin American Museum of Natural History*, 244, 1–306. [https://doi.org/10.1206/0003-0090\(2000\)244%3C0001:MOTRJA%3E2.0.CO;2](https://doi.org/10.1206/0003-0090(2000)244%3C0001:MOTRJA%3E2.0.CO;2)
- 678 Patton, J. L., Pardiñas, U. F. J., & D'Elia, G. (2015). *Mammals of South America, Volume 2, Rodents*. The University of Chicago Press.

- 679 Peterson, B. K., Weber, J. N., Kay, E. H., Fisher, H. S., & Hoekstra, H. E. (2012). Double digest RADseq: an inexpensive method for *de novo* SNP
680 discovery and genotyping in model and non-model species. *PLoS ONE*, 7(5), e37135. <https://doi.org/10.1371/journal.pone.0037135>
- 681 Pinheiro, J., Bates, D., DebRoy, S., & Sarkar, D. (2020). *nlme: linear and nonlinear mixed effects models*. <https://cran.r-project.org/package=nlme>
- 682 Pirani, R. M., Werneck, F. P., Thomaz, A. T., Kenney, M. L., Sturaro, M. J., Ávila-Pires, T. C. S., ... Knowles, L. L. (2019). Testing main Amazonian
683 rivers as barriers across time and space within widespread taxa. *Journal of Biogeography*, 46(11), 2444–2456. <https://doi.org/10.1111/jbi.13676>
- 684 Pope, N. (2020). *r2vcftools: An R interface for vcftools. R package version 0.0.0.9000*.
- 685 Prado, J. R., Percequillo, A. R., Thomaz, A. T., & Knowles, L. L. (2019). Similar but different: Revealing the relative roles of species-traits versus biome
686 properties structuring genetic variation in South American marsh rats. *Journal of Biogeography*, 46(4), 770–783. <https://doi.org/10.1111/jbi.13529>
- 687 Puechmaile, S. J. (2016). The program structure does not reliably recover the correct population structure when sampling is uneven: subsampling and new
688 estimators alleviate the problem. *Molecular Ecology Resources*, 16(3), 608–627. <https://doi.org/10.1111/1755-0998.12512>
- 689 R Core Team. (2020). *R: A language and environment for statistical computing*. R Foundation for Statistical Computing. <https://www.r-project.org/>
- 690 Ribas, C. C., Aleixo, A., Nogueira, A. C. R., Miyaki, C. Y., & Cracraft, J. (2012). A palaeobiogeographic model for biotic diversification within Amazonia
691 over the past three million years. *Proceedings of the Royal Society of London B: Biological Sciences*, 279(1729), 681–689,
692 <https://doi.org/10.1098/rspb.2011.1120>.
- 693 Rutten, A., Cox, K., Scheppers, T., Broecke, V., Leirs, H., Casaer, J., ... Leirs, H. (2019). Analysing the recolonisation of a highly fragmented landscape by
694 wild boar using a landscape genetic approach. *Wildlife Biology*, 2019(1), 1–11. <https://doi.org/10.2981/wlb.00542>
- 695 Salo, J., Kalliola, R., Häkkinen, I., Mäkinen, Y., Niemelä, P., Puhakka, M., & Coley, P. D. (1986). River dynamics and the diversity of Amazon lowland
696 forest. *Nature*, 322(6076), 254–258. <https://doi.org/10.1038/322254a0>
- 697 Shirk, A. J., Landguth, E. L., & Cushman, S. A. (2017). A comparison of individual-based genetic distance metrics for landscape genetics. *Molecular*
698 *Ecology Resources*, 17(6), 1308–1317. <https://doi.org/10.1111/1755-0998.12684>
- 699 Shirk, A. J., Landguth, E. L., & Cushman, S. A. (2018). A comparison of regression methods for model selection in individual-based landscape genetic
700 analysis. *Molecular Ecology Resources*, 18(1), 55–67. <https://doi.org/10.1111/1755-0998.12709>
- 701 Sikes, R. S. (2016). 2016 Guidelines of the American Society of Mammalogists for the use of wild mammals in research and education. *Journal of*
702 *Mammalogy*, 97(3), 663–688. <https://doi.org/10.1093/jmammal/gyw078>
- 703 Silk, M. J., Harrison, X. A., & Hodgson, D. J. (2020). Perils and pitfalls of mixed-effects regression models in biology. *PeerJ*, 8, e9522.
704 <https://doi.org/10.7717/peerj.9522>
- 705 Smith, B. T., McCormack, J. E., Cuervo, A. M., Hickerson, M. J., Aleixo, A., Cadena, C. D., ... Brumfield, R. T. (2014). The drivers of tropical speciation.
706 *Nature*, 515(7527), 406–409. <https://doi.org/10.1038/nature13687>
- 707 Taylor, P. D., Fahrig, L., Henein, K., & Merriam, G. (1993). Connectivity is a vital element of landscape structure. *Oikos*, 68(3), 571–573.
708 <https://doi.org/10.2307/3544927>
- 709 Thom, G., Xue, A. T., Sawakuchi, A. O., Ribas, C. C., Hickerson, M. J., Aleixo, A., & Miyaki, C. (2020). Quaternary climate changes as speciation drivers
710 in the Amazon floodplains. *Science Advances*, 6(11), eaax4718. <https://doi.org/10.1126/sciadv.aax4718>
- 711 Tracy, C. A., & Widom, H. (1994). Level spacing distributions and the Bessel kernel. *Communications in Mathematical Physics*, 161(2), 289–309.
712 <https://doi.org/10.1007/BF02099779>
- 713 van Soelen, E. E., Kim, J.-H., Santos, R. V., Dantas, E. L., Vasconcelos de Almeida, F., Pires, J. P., ... Sinninghe Damsté, J. S. (2017). A 30 Ma history of
714 the Amazon River inferred from terrigenous sediments and organic matter on the Ceará Rise. *Earth and Planetary Science Letters*, 474, 40–48.
715 <https://doi.org/10.1016/J.EPSL.2017.06.025>
- 716 Vormisto, J., Tuomisto, H., & Oksanen, J. (2004). Palm distribution patterns in Amazonian rainforests: What is the role of topographic variation? *Journal*
717 *of Vegetation Science*, 15(4), 485–494. <https://doi.org/10.1111/j.1654-1103.2004.tb02287.x>
- 718 Voss, R. S., & Emmons, L. H. (1996). Mammalian diversity in Neotropical lowland rainforests: a preliminary assessment. *Bulletin of the American*
719 *Museum of Natural History*, 230, 1–115.
- 720 Voss, R. S., Lunde, D. P., & Simmons, N. B. (2001). The mammals of Paracou, French Guiana: a Neotropical lowland rainforest fauna part 2. Nonvolant
721 species. *Bulletin of the American Museum of Natural History*, 263, 3–236. [https://doi.org/10.1206/0003-0090\(2001\)263<0003:TMOPFG>2.0.CO;2](https://doi.org/10.1206/0003-0090(2001)263<0003:TMOPFG>2.0.CO;2)
- 722
- 723 Wittmann, F., Schöngart, J., & Junk, W. J. (2010). Phytogeography, species diversity, community structure and dynamics of Central Amazonian floodplain
724 forests. In Wolfgang J. Junk, M. T. F. Piedade, F. Wittmann, J. Schöngart, & P. Parolin (Eds.), *Amazonian floodplain forests: ecophysiology,*
725 *biodiversity and sustainable management* (pp. 61–102). Springer.
- 726 Woods, & Kilpatrick. (2005). Infraorder Hystricognathi Brandt, 1855. In D. E. Wilson & D. M. Reeder (Eds.), *Mammal Species of the World. A*
727 *Taxonomic and Geographic Reference* (Volume 2, pp. 1538–1600). Johns Hopkins University Press.

- 728 Wright, S. (1943). Isolation by Distance. *Genetics*, 28(2), 114–138. <http://www.ncbi.nlm.nih.gov/pubmed/17247074>
- 729 Yang, J., Benyamin, B., McEvoy, B. P., Gordon, S., Henders, A. K., Nyholt, D. R., ... Visscher, P. M. (2010). Common SNPs explain a large proportion of
730 the heritability for human height. *Nature Genetics*, 42(7), 565–569. <https://doi.org/10.1038/ng.608>

731

732

733 BIOSKETCH

734 The authors share an interest in the study of processes that structure the genetic variation among taxa and across geography.

735 JD: designed and performed the experiments, gathered and analyzed the data, wrote the manuscript and made the figures

736 and tables; JRP: designed the experiments, provided analysis tools, and contributed to writing of the manuscript; ARP:

737 designed the experiments, provided reagents/materials/analysis tools, and contributed to writing the manuscript; LLK:

738 designed the experiments, provided reagents/materials/analysis tools, and contributed to writing the manuscript.

739

740 **Editor:** Fabricio Villalobos.

Tables

Table 1: The best fit models ($\Delta AIC < 2$ with the best fit model in bold) for observed geographic distribution of relatedness coefficients in *P. simonsi* (the non-flooded forest/terra-firme species) and in *P. steerei*, (the seasonal floodplain forests/várzea species) using MLPE. The contribution of each predictor variable (and standard error, in parentheses) calculated with REML (see Material and Methods for details) are shown, as the significance of chi-squared contingency table tests each predictor in the models, with * for $p < 0.05$, ** for $p < 0.01$, ^{ns} if not significant. There was no statistically significant difference in the fit of the best models (in bold) for *P. simonsi* species and the other models using the likelihood-ratio tests (LRT) in p-value column. Log-likelihoods (logL), and correlation coefficient, ρ , between relatedness coefficients and distances specified by each model. The conditional R^2 and its confidence intervals in parenthesis (a measure of variance explained by the entire model, including fixed and random effects) are also shown for the best fit models. Results for all models taking into account the correlations among the predictors variables (i.e., the uncorrelated models) are presented in Tables S1.12-S1.13.

Models	Habitat	Productivity	River	logL	ρ	Conditional R^2 (C.I. 95%)	p-value
P. simonsi:							
Habitat** + Productivity ^{ns}	-0.091 (0.015)	-0.020 (0.017)	.	58.698	0.048		0.149
Habitat**	-0.098 (0.013)	.	.	60.767	0.028	0.349 (0.233 – 0.467)	.
Habitat** + River ^{ns}	-0.095 (0.015)	.	-0.008 (0.015)	57.568	0.026		0.597
Habitat** + Productivity ^{ns} + River ^{ns}	-0.092 (0.016)	-0.021 (0.019)	0.003 (0.016)	55.577	0.050		0.345
P. steerei:							
Habitat** + River**	-0.032 (0.006)	.	-0.111 (0.008)	163.332	0.469	0.668 (0.732 – 0.599)	.

80°W

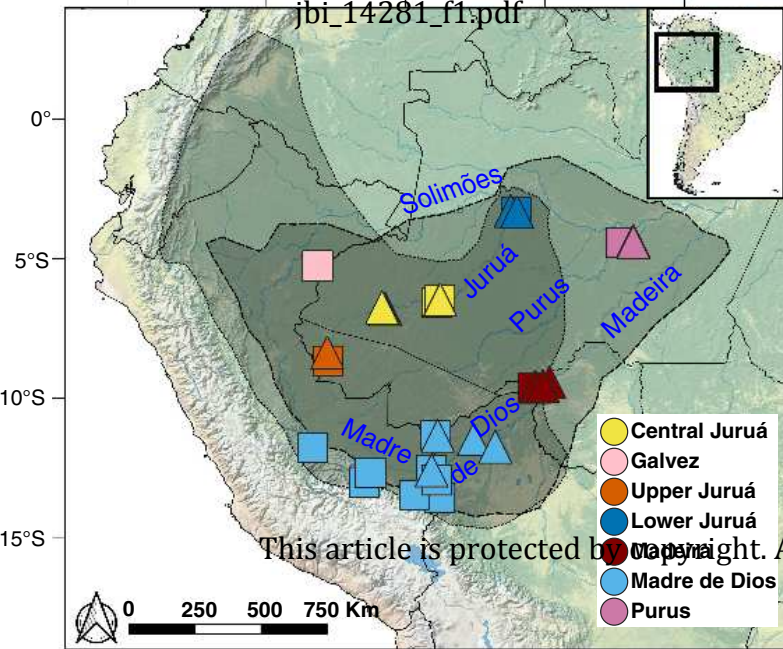
75°W

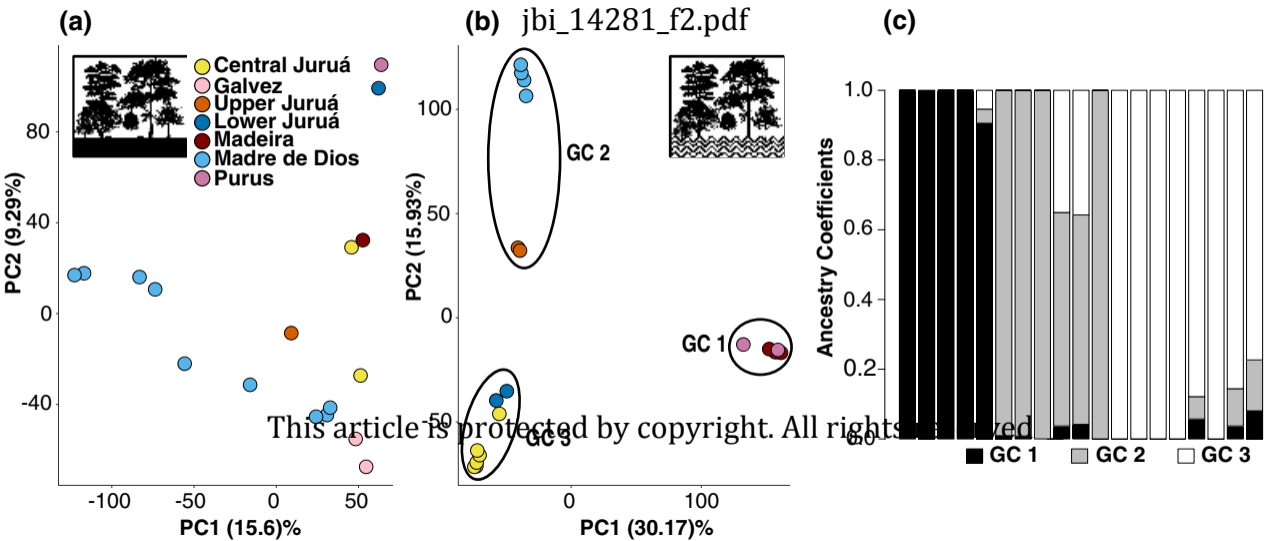
70°W

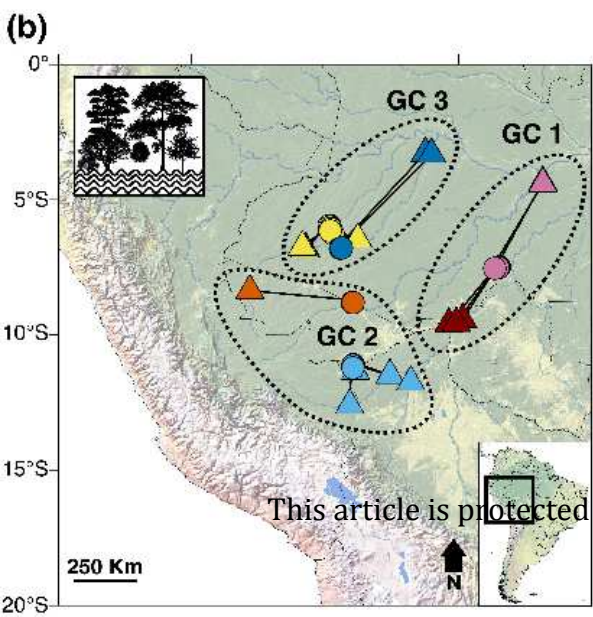
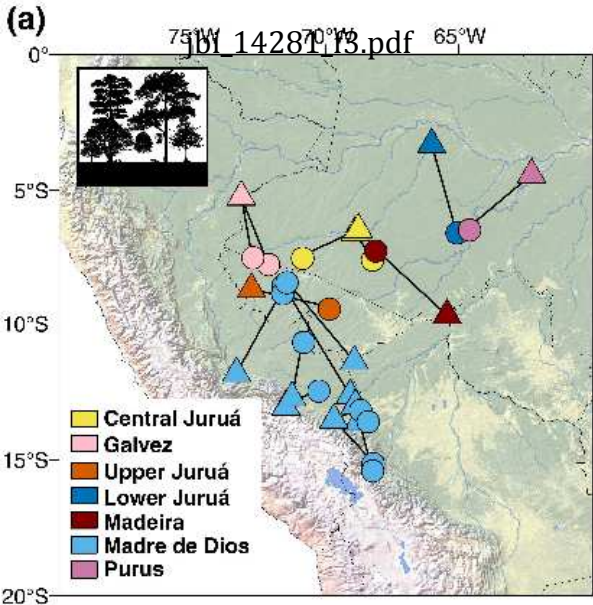
65°W

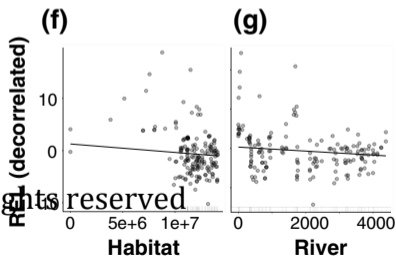
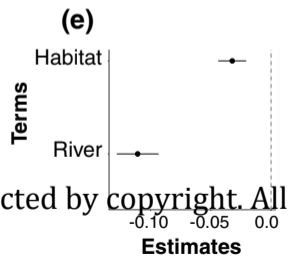
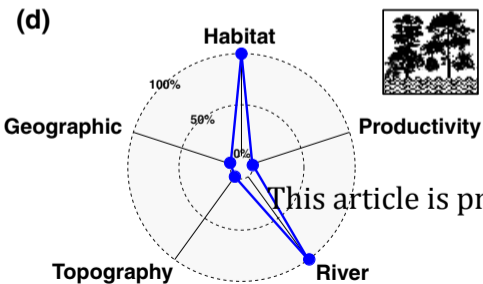
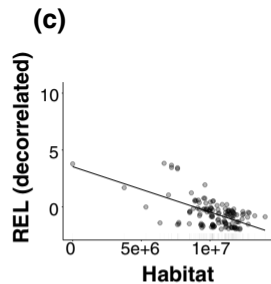
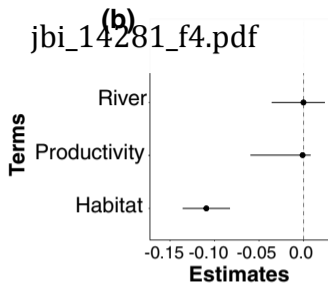
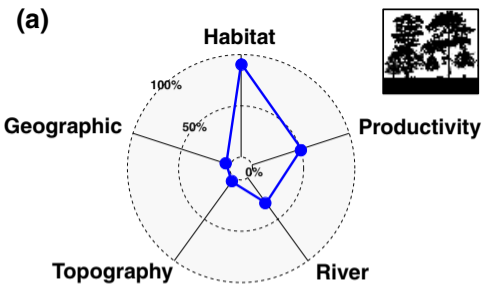
60°W

jbi_14281_f1.pdf









This article is protected by copyright. All rights reserved